

# Testing cosmic anisotropy with the Combo correlation of gamma-ray bursts

Dong Zhao<sup>1</sup>, Hao-Ran Duan<sup>1</sup>, Jun-Qing Xia<sup>2,3\*</sup>

<sup>1</sup>Center for Gravitation and Cosmology, College of Physical Science and Technology, Yangzhou University, Yangzhou, 225009, China.

<sup>2</sup>Institute for Frontiers in Astronomy and Astrophysics, Beijing Normal University, Beijing, 100875, China.

<sup>3</sup>School of Physics and Astronomy, Beijing Normal University, Beijing, 100875, China.

\*Corresponding author(s). E-mail(s): [xiajq@bnu.edu.cn](mailto:xiajq@bnu.edu.cn);

## Abstract

We employ the sample of 244 gamma-ray bursts (GRBs; i.e., C244) with the Combo correlation to test cosmic anisotropy. Meanwhile, the Pantheon sample is introduced to verify whether the GRB sample can suppress the fake anisotropic signals induced by inhomogeneous spatial distributions. In the dipole fitting (DF) method, under the dipole-modulated  $\Lambda$ CDM model, the C244 sample shifts the best-fitting longitude  $l$  derived from the Pantheon sample by  $54.09^\circ$  and reduces the uncertainty in  $l$  by approximately 40%. Compared to the 118 GRBs (i.e., A118) with the  $E_p$ - $E_{\text{iso}}$  correlation, the shift in longitude  $l$  increases by additional  $21.35^\circ$ . In the hemisphere comparison (HC) method, the preferred direction derived from the C244+Pantheon sample deviates from that of the Pantheon-only sample by more than  $1\sigma$ . In contrast, the preferred direction from the A118+Pantheon sample is consistent with the Pantheon-only result within the  $1\sigma$  uncertainty. The preferred direction changes significantly as the number of GRBs increases from 118 to 244. Our results show that a larger GRB sample can reduce the fake anisotropic signals caused by inhomogeneous spatial distributions. Accordingly, we suggest that GRBs have the potential to provide a reliable probe of cosmic anisotropy.

## 1 Introduction

The theoretical framework of modern cosmology is based on the cosmological principle, which assumes that the Universe exhibits homogeneity and isotropy at large scales. Observations of the cosmic microwave background (CMB) radiation by the Wilkinson Microwave Anisotropy Probe (WMAP) [1] and Planck satellites [2] have confirmed its validity with high precision. However, several anomalies emerge from current observations, posing a potential challenge to the cosmological principle. These include the hemispherical

power asymmetry [3] and the parity asymmetry [4–6] in the CMB, as well as the large-scale alignment of quasar polarization vectors [7, 8]. These anomalies suggest that the Universe may have a preferred direction.

As standard candles in cosmology, datasets of Type Ia supernovae (SNe Ia) have been extensively used to test the cosmological principle. These datasets include Union2 [9] and 2.1 [10], JLA [11], Pantheon [12], and Pantheon+ [13]. Studies have shown that although a dipole signal with  $2\sigma$  statistical significance was detected in the Union2 [14, 15] and 2.1 [16–19] datasets, this

dipole signal has not been confirmed in subsequent JLA [20–22], Pantheon [23–26], and Pantheon+ [27] datasets. However, some studies have pointed out that a significant dipole signal can still be detected in the low-redshift subsample of the Pantheon+ sample [27–31]. Furthermore, when analyzed using the HC method, both the Pantheon [25] and Pantheon+ [32, 33] datasets exhibited significant anisotropic signals. There is a sharp change in the anisotropy level of the Pantheon+ sample occurring at distances less than  $40Mpc$  [34]. It is also worth noting that some studies suggest that the Pantheon+ sample are consistent with the isotropic assumption [35, 36].

In addition to SNe Ia datasets, other types of cosmological observations are also widely used to test cosmic anisotropy. An incomplete list of related works includes galaxies [37, 38], galaxy clusters [39–43], gravitational waves [44–47], fast radio bursts [44, 48, 49], the sky distribution of radio and infrared sources [50–63], quasars [64–66], and GRBs [67–73].

Some studies suggest that anisotropic signals may stem from the inhomogeneous spatial distribution of datasets in the sky. Zhao et al. [25] discovered that the anisotropic signals detected in the Pantheon sample are heavily dependent on the inhomogeneous distribution of SNe Ia in the sky. Sun and Wang [19] found that the anisotropic distribution of coordinates can cause the dipole direction to change and increase the magnitude of the dipole. Therefore, the search for convincing anisotropic signals requires observational datasets with a more uniform spatial distribution.

The spatial distribution of quasar samples [74–76] is more uniform than that of the Pantheon sample. Some studies have used quasar samples to investigate anisotropic signals [64–66]. However, it should be noted that the “more uniform” spatial distribution of quasar samples is only relative to the Pantheon sample. The quasar samples still exhibit significant spatial inhomogeneities. For the 2020 compilation of quasars [76], almost 70% of quasars are located in the northern galactic hemisphere, and the rest are concentrated in the southeastern galactic hemisphere, meaning that their spatial distribution remains highly inhomogeneous. In contrast, GRBs are the most powerful explosions observed in the universe, with a redshift range extending up to  $z = 9.4$  [77, 78]. The peak of their redshift distribution is almost at the

maximum redshift of SNe Ia [79]. More importantly, the spatial distribution of GRBs is nearly homogeneous.

Previously, we tested cosmic anisotropy with the  $E_p$ - $E_{\text{iso}}$  (‘Amati’) correlation [80] of 118 long GRBs [81, 82]. We found that although the number of GRBs is only about a tenth of the Pantheon sample size, they can considerably impact the anisotropic signals arising from the inhomogeneous sky distribution of the Pantheon sample [71]. In this work, we will analyze a larger sample of 244 GRBs [83] with the Combo correlation [84, 85]. We will perform a joint analysis by combining the Pantheon sample with these 244 GRBs. Because the anisotropic signals in the Pantheon sample stem from the uneven spatial distribution of its data across the sky [25], it serves as an ideal tool to test whether introducing a more homogeneously distributed dataset can suppress these signals. We will investigate the impact of expanding the GRB sample size from 118 to 244 on the anisotropic signals in the Pantheon sample. The rest of this paper is organized as follows. In Section 2, we briefly introduce the 244 GRBs and the Combo correlation. In Section 3, we employ the DF and HC methods to investigate cosmic anisotropy. Finally, conclusions and discussions are presented in Section 4.

## 2 Methodology

### 2.1 The GRB sample

The 244 GRBs [83] used in our work span a redshift range of  $0.0331 \leq z \leq 9.4$ . Fig. 1 displays their redshift distribution (orange histogram). For comparison, we also show the redshift distribution of the A118 sample used in our previous work [71] in Fig. 1 with the blue histogram. Most C244 sources are concentrated within  $0 < z < 4$ . The C244 sample exhibits a higher density of GRBs in the redshift range  $0 < z < 3$ , and extends up to  $z = 9.4$ . The redshift distribution of the Pantheon sample is shown in Fig. 2. We show the spatial distributions of the C244, A118, and Pantheon samples in Fig. 3. The C244 and A118 samples are both nearly uniformly distributed in the sky. In contrast, the Pantheon sample is highly inhomogeneous, with approximately 335 sources concentrated in a distinct band along the celestial equator.

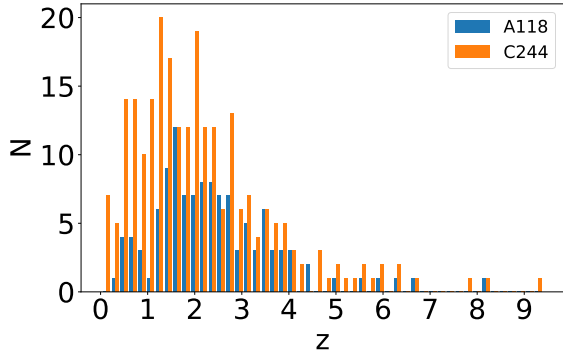


**Fig. 1:** Redshift distribution of the GRB samples. The blue histogram denotes the A118 sample [81, 82], while the orange histogram represents the C244 sample [83].

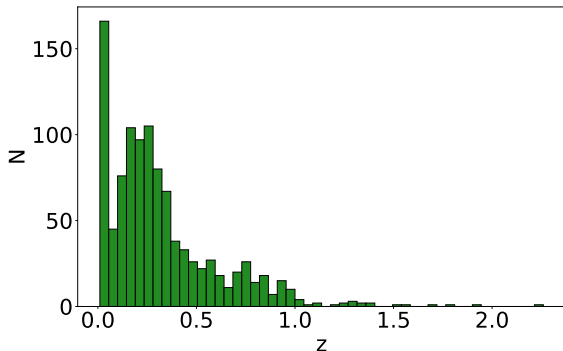


**Fig. 2:** Redshift distribution of the Pantheon sample.

## 2.2 The Combo correlation

The Combo correlation [84, 85] is an empirical relationship that combines prompt and afterglow emissions in long GRBs, expressed as

$$\log\left(\frac{L_0}{\text{erg/s}}\right) = \alpha + \beta \log\left(\frac{E_p}{\text{keV}}\right) - \log\left(\frac{T}{\text{s}}\right), \quad (1)$$

where  $\log$  denotes  $\log_{10}$ .  $\alpha$  and  $\beta$  are two free parameters determined by the C244 sample.  $E_p$  is the rest-frame peak energy of the GRB photon energy spectrum.  $T$  is the X-ray afterglow rest-frame effective duration of the plateau phase, and  $L_0$  represents the X-ray afterglow plateau

luminosity, which can be derived from

$$L_0 = 4\pi d_L^2(z) F_0, \quad (2)$$

where  $F_0$  denotes the X-ray afterglow flux in the rest frame. The luminosity distance  $d_L$  has the form

$$d_L = \frac{c(1+z)}{H_0} \int_0^z \frac{dz'}{E(z')}, \quad (3)$$

$z$  represents the redshift of sources, and  $c$  is the speed of light.  $H_0$  denotes the Hubble constant. In this work,  $H_0$  is fixed to  $70 \text{ km s}^{-1} \text{ Mpc}^{-1}$ . In the flat  $\Lambda$ CDM model,  $E(z)$  is given as

$$E(z) = \sqrt{\Omega_m(1+z)^3 + (1 - \Omega_m)}, \quad (4)$$

where  $\Omega_m$  is the matter density.

The  $\chi^2$  of the GRB sample can be formulated as [86]

$$\chi_{\text{GRB}}^2 = \sum_{i=1}^{N_{\text{GRB}}} \left[ \frac{(\log L_{0,i}^{\text{th}} - \log L_{0,i}^{\text{obs}})^2}{s_i^2} + \ln(2\pi s_i^2) \right], \quad (5)$$

where  $s_i^2$  is computed via

$$s_i^2 = \sigma_{\log F_{0,i}}^2 + \beta^2 \sigma_{\log E_{p,i}}^2 + \sigma_{\log T_i}^2 + \sigma^2, \quad (6)$$

where  $\sigma_{\log F_0}$ ,  $\sigma_{\log E_p}$ , and  $\sigma_{\log T}$  represent the uncertainties of  $\log F_0$ ,  $\log E_p$ , and  $\log T$ , respectively.  $\sigma$  denotes systematics and additional hidden uncertainties.

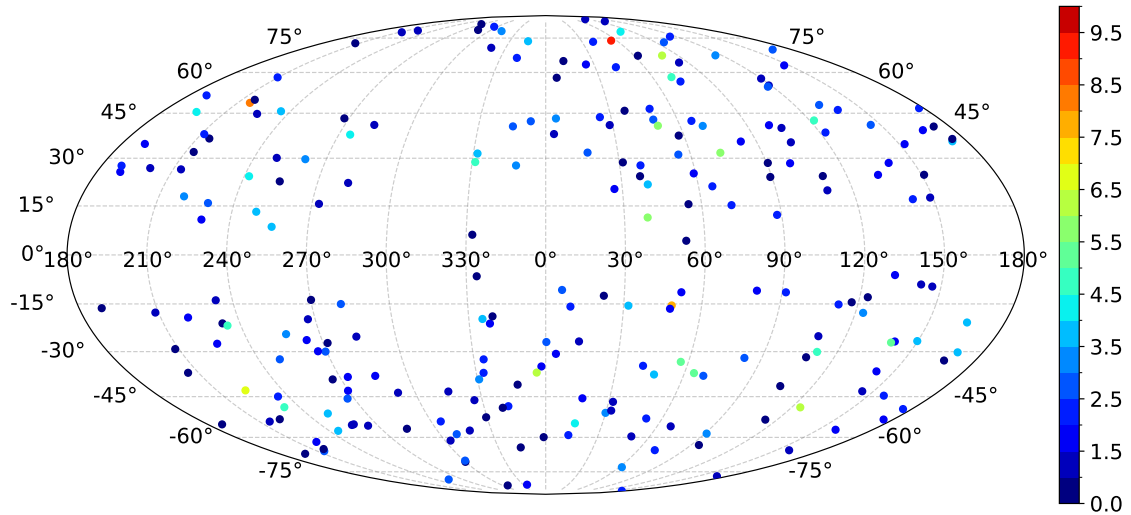
## 2.3 The dipole fitting method

Mariano and Perivolaropoulos [14] proposed the DF method. It is now widely used to test cosmic anisotropy. In this work, we employ a distance modulus modified by a dipole modulation, expressed as

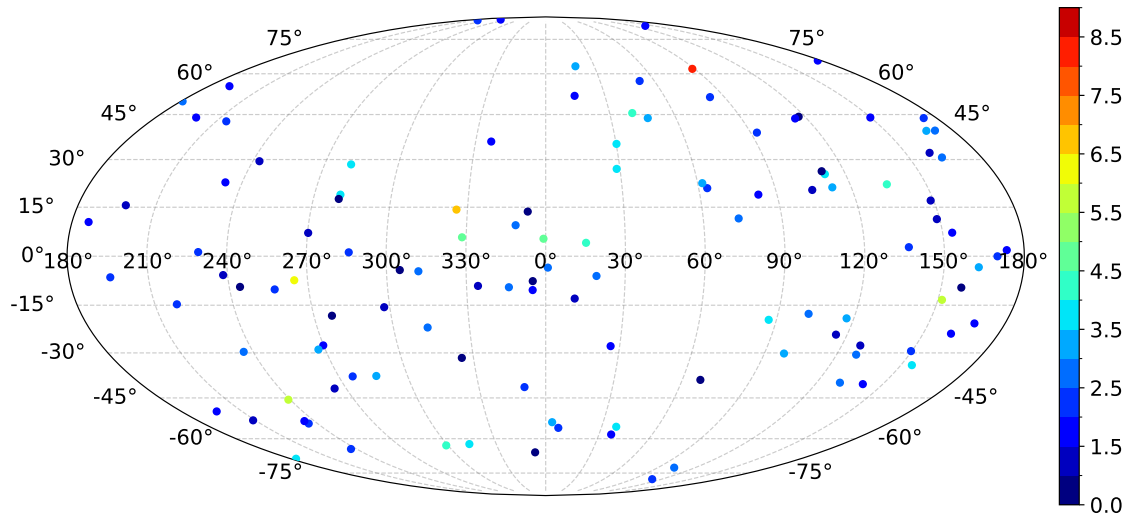
$$\tilde{\mu}_{\text{th}} = \mu_{\text{th}} \times (1 + A_D(\hat{\mathbf{n}} \cdot \hat{\mathbf{p}})), \quad (7)$$

where  $\hat{\mathbf{n}}$  is the dipole direction and  $\hat{\mathbf{p}}$  is the unit vector pointing to the position of the sources.  $A_D$  denotes the dipole amplitude. In Galactic coordinates, the dipole direction  $\hat{\mathbf{n}}$  is parameterized as

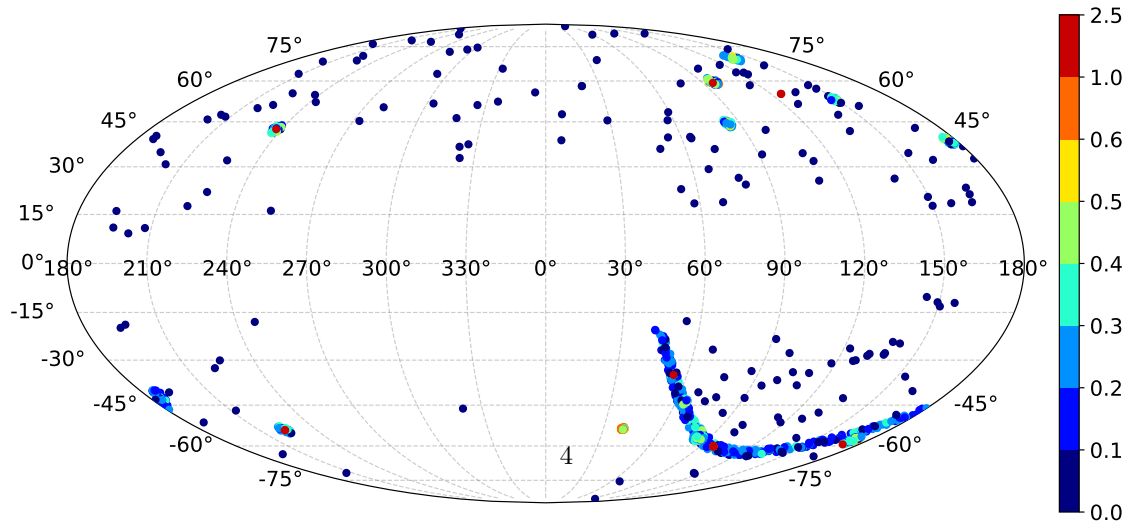
$$\hat{\mathbf{n}} = \cos(b) \cos(l) \hat{\mathbf{i}} + \cos(b) \sin(l) \hat{\mathbf{j}} + \sin(b) \hat{\mathbf{k}}, \quad (8)$$



(a) C244 sample



(b) A118 sample



(c) Pantheon sample

**Fig. 3:** Distributions of the GRB samples and the Pantheon sample in Galactic coordinates, where the pseudo-colors represent the redshift of the sources.

where  $l$  and  $b$  denote the Galactic longitude and latitude of the dipole direction, respectively.  $\hat{i}$ ,  $\hat{j}$ , and  $\hat{k}$  are the standard Cartesian unit vectors. The unit vector  $\hat{\mathbf{p}}$  points to the  $i$ -th source, taking the form

$$\hat{\mathbf{p}}_i = \cos(b_i) \cos(l_i) \hat{i} + \cos(b_i) \sin(l_i) \hat{j} + \sin(b_i) \hat{k}. \quad (9)$$

In the  $\Lambda$ CDM model, the theoretical distance modulus is given by

$$\mu_{\text{th}} = 5 \log \frac{d_L}{\text{Mpc}} + 25, \quad (10)$$

By combining Eqs. (7) and (10), we derive the expression for the luminosity distance under dipole modulation, expressed as

$$\log \frac{\tilde{d}_L}{\text{Mpc}} = \left( \log \frac{d_L}{\text{Mpc}} + 5 \right) \times (1 + A_D (\hat{\mathbf{n}} \cdot \hat{\mathbf{p}})) - 5, \quad (11)$$

plugging Eq. (11) into Eq. (2), we obtain the expression for the X-ray afterglow plateau luminosity  $L_0$  under dipole modulation.

In addition to the dipole-modulated  $\Lambda$ CDM model, we also explore the Finslerian cosmological model [17] in our analysis. The dipole structure is naturally given in the expression of  $E(z)$ , which takes the form

$$E(z) = \sqrt{\Omega_m (1+z)^3 (1 + A_D \cos \theta)^{-3} + 1 - \Omega_m}, \quad (12)$$

where  $A_D$  denotes the dipole amplitude and  $\theta$  is the angle between the dipole direction and the position of the sources.

## 2.4 The hemisphere comparison method

Schwarz and Weinhorst [87] originally introduced the HC method to probe cosmic anisotropy. The steps of the HC method can be summarized as:

(1) Generate a random direction  $\hat{\mathbf{n}}(l, b)$  in Galactic coordinates, where  $l$  and  $b$  represent the Galactic longitude and latitude, respectively. Given this random direction  $\hat{\mathbf{n}}$ , the celestial sphere is divided into two distinct “up” and “down” hemispheres.

(2) Based on the sources’ coordinates, the sample can be divided into two subsets corresponding to the “up” and “down” hemispheres, respectively.

(3) Find the best-fitting value of  $\Omega_m$  and its  $1\sigma$  uncertainty for each subset assuming a flat  $\Lambda$ CDM model. The anisotropy level (AL) is defined as

$$\text{AL} = 2 \times \frac{\Omega_{\text{m,u}} - \Omega_{\text{m,d}}}{\Omega_{\text{m,u}} + \Omega_{\text{m,d}}}, \quad (13)$$

where the subscript  $u$  denotes the “up” hemisphere and the subscript  $d$  denotes the “down” hemisphere. The  $1\sigma$  uncertainty of AL is given by

$$\sigma_{\text{AL}} = \frac{\sqrt{\sigma_{\Omega_{\text{m,u}}}^2 + \sigma_{\Omega_{\text{m,d}}}^2}}{\Omega_{\text{m,u}} + \Omega_{\text{m,d}}}. \quad (14)$$

(4) Repeat the above steps to generate adequate directions. Find the maximum AL (i.e.,  $\text{AL}_{\text{max}}$ ) and its corresponding direction.

## 3 Results

### 3.1 Dipole fitting

The full parameter space is explored via the Markov Chain Monte Carlo (MCMC) method using the Python package `emcee`<sup>1</sup> [88]. The flat priors for the free parameters in this work are set as follows:  $\Omega_m \in [0.2, 0.4]$ ,  $\alpha \in [48, 51]$ ,  $\beta \in [0.5, 1.1]$ ,  $\sigma \in [0.25, 0.5]$ ,  $A_D \in [0, 1]$ ,  $l \in [0^\circ, 360^\circ]$ ,  $b \in [-90^\circ, 90^\circ]$ ,  $\mathcal{M} \in [23.5, 24]$ . We present the results in Figs. 4 and 5, and summarize them in Table 1. To avoid redundancy, we do not show the results of the nuisance parameter  $\mathcal{M}$  from the Pantheon sample.

In the dipole-modulated  $\Lambda$ CDM model, the Combo correlation constraints from the C244 sample are determined to be  $\alpha = 49.854^{+0.133}_{-0.173}$ ,  $\beta = 0.785^{+0.060}_{-0.058}$ , and  $\sigma = 0.373^{+0.023}_{-0.020}$ . The dipole amplitude  $A_D$  yields an upper limit of  $A_D < 1.241 \times 10^{-3}$  at the 95% CL, implying that the dipole anisotropy is very weak. Additionally, the dipole direction points toward  $(l, b) = (232.49^{+57.18^\circ}_{-56.96^\circ}, -8.33^{+36.73^\circ}_{-47.86^\circ})$ . For the Finslerian

<sup>1</sup><https://emcee.readthedocs.io/en/stable/>

**Table 1:** Best-fit parameters with 68% confidence level (CL) are summarized for the dipole-modulated  $\Lambda$ CDM model and the Finslerian cosmological model. For parameters with only an upper or lower bound, the 95% CL is reported instead.

Model	Data	$\Omega_m$	$\alpha$	$\beta$	$\sigma$	$10^3 A_D$	$l[^\circ]$	$b[^\circ]$
$\Lambda$ CDM	C244	—	$49.854^{+0.133}_{-0.173}$	$0.785^{+0.060}_{-0.058}$	$0.373^{+0.023}_{-0.020}$	$< 1.241$	$232.49^{+57.18}_{-56.96}$	$-8.33^{+36.73}_{-47.86}$
	C244+Pantheon	$0.318^{+0.018}_{-0.025}$	$49.840^{+0.154}_{-0.151}$	$0.789^{+0.066}_{-0.053}$	$0.380^{+0.018}_{-0.024}$	$< 0.891$	$255.01^{+56.83}_{-80.27}$	$-29.13^{+21.53}_{-45.30}$
	Pantheon	$0.296^{+0.024}_{-0.020}$	—	—	—	$< 1.142$	$309.10^{+86.30}_{-125.40}$	$-33.65^{+15.28}_{-56.02}$
	A118+Pantheon	$0.298^{+0.022}_{-0.022}$	—	—	—	$< 1.128$	$276.36^{+56.04}_{-77.33}$	$-37.30^{+20.49}_{-40.93}$
Finslerian	C244	—	$49.841^{+0.154}_{-0.158}$	$0.794^{+0.050}_{-0.070}$	$0.375^{+0.021}_{-0.022}$	$< 145.741$	$249.43^{+55.27}_{-75.27}$	$-12.20^{+39.94}_{-50.82}$
	C244+Pantheon	$0.314^{+0.020}_{-0.023}$	$49.841^{+0.150}_{-0.159}$	$0.802^{+0.056}_{-0.063}$	$0.380^{+0.018}_{-0.024}$	$< 18.916$	$301.47^{+56.55}_{-140.83}$	$-26.43^{+14.91}_{-56.66}$
	Pantheon	$0.296^{+0.022}_{-0.022}$	—	—	—	$< 19.181$	$305.45^{+57.44}_{-148.38}$	$-35.46^{+19.96}_{-50.27}$
	A118+Pantheon	$0.297^{+0.024}_{-0.020}$	—	—	—	$< 20.251$	$301.83^{+61.21}_{-133.36}$	$-33.64^{+23.20}_{-45.35}$

cosmological model, the results for the parameters in the Combo correlation are almost identical to those obtained in the dipole-modulated  $\Lambda$ CDM model. A negligible dipole anisotropy is observed, with an upper limit of  $A_D < 0.146$  at the 95% CL. The dipole direction is  $(l, b) = (249.43^{+55.27^\circ}_{-75.27^\circ}, -12.20^{+39.94^\circ}_{-50.82^\circ})$ .

We combine the C244 sample with the Pantheon sample to obtain joint cosmological constraints. In the dipole-modulated  $\Lambda$ CDM model, the Combo correlation constraints from the joint dataset are determined to be  $\alpha = 49.840^{+0.154}_{-0.151}$ ,  $\beta = 0.789^{+0.066}_{-0.053}$ , and  $\sigma = 0.380^{+0.018}_{-0.024}$ . The matter density  $\Omega_m$  is  $0.318^{+0.018}_{-0.025}$ . The dipole amplitude  $A_D$  yields an upper limit of  $A_D < 0.891 \times 10^{-3}$  at the 95% CL and the dipole direction points to  $(l, b) = (255.01^{+56.83^\circ}_{-80.27^\circ}, -29.13^{+21.53^\circ}_{-45.30^\circ})$ . For the Finslerian cosmological model, the results of the parameters in the Combo correlation are almost identical to those mentioned above. The matter density  $\Omega_m$  is  $0.314^{+0.020}_{-0.023}$ . The dipole amplitude  $A_D$  yields an upper limit of  $A_D < 0.019$  at the 95% CL, with the corresponding direction pointing to  $(l, b) = (301.47^{+56.55^\circ}_{-140.83^\circ}, -26.43^{+14.91^\circ}_{-56.66^\circ})$ .

Figure 6 displays the anisotropic signals derived from the C244+Pantheon, A118+Pantheon, and Pantheon samples. The results for the A118+Pantheon sample, which are also shown in Table 1, are taken from our previous work [71]. The results indicate that the dipole amplitudes for all datasets are small, suggesting that the anisotropic signals in these datasets are very weak. In the dipole-modulated  $\Lambda$ CDM model, when the Pantheon sample is combined

with the two GRB samples, respectively, the results for the Galactic longitude  $l$  show obvious changes. The uncertainty in the longitude  $l$  is reduced by approximately 40%. The addition of the A118 sample induces a shift of  $32.74^\circ$  in the longitude  $l$ . With approximately twice the sample size of the A118 sample, the C244 sample shifts the longitude  $l$  by  $54.09^\circ$ . Additionally, under the Finslerian cosmological model, the dipole directions determined from these three datasets are highly consistent with each other.

### 3.2 Hemisphere comparison

In the HC method, we use the Python package `healpy`<sup>2</sup> [89, 90] to generate random directions with  $N_{\text{side}} = 128$ . The total number of random directions is  $12 \times N_{\text{side}}^2 = 196,608$ . In the analysis, we fix the Combo correlation parameters at  $\alpha = 49.80$ ,  $\beta = 0.791$ , and  $\sigma = 0.375$ . These values are adopted from the flat  $\Lambda$ CDM model. The C244 sample is combined with the Pantheon sample to obtain joint cosmological constraints. We minimize  $\chi^2 = \chi_{\text{GRB}}^2 + \chi_{\text{Pantheon}}^2$  to determine the best-fitting  $\Omega_m$  and its  $1\sigma$  uncertainty for the subsets corresponding to the “up” and “down” hemispheres. Figure 7 shows the pseudo-color map of AL from the C244+Pantheon sample in Galactic coordinates. The  $AL_{\text{max}}$  is  $0.264 \pm 0.057$  and the corresponding direction is  $(l, b) = (66.45^{+31.29^\circ}_{-51.68^\circ}, -9.59^{+53.00^\circ}_{-17.69^\circ})$ . In the preferred direction, the best-fitting values of  $\Omega_m$  in

<sup>2</sup><http://healpix.sourceforge.net>

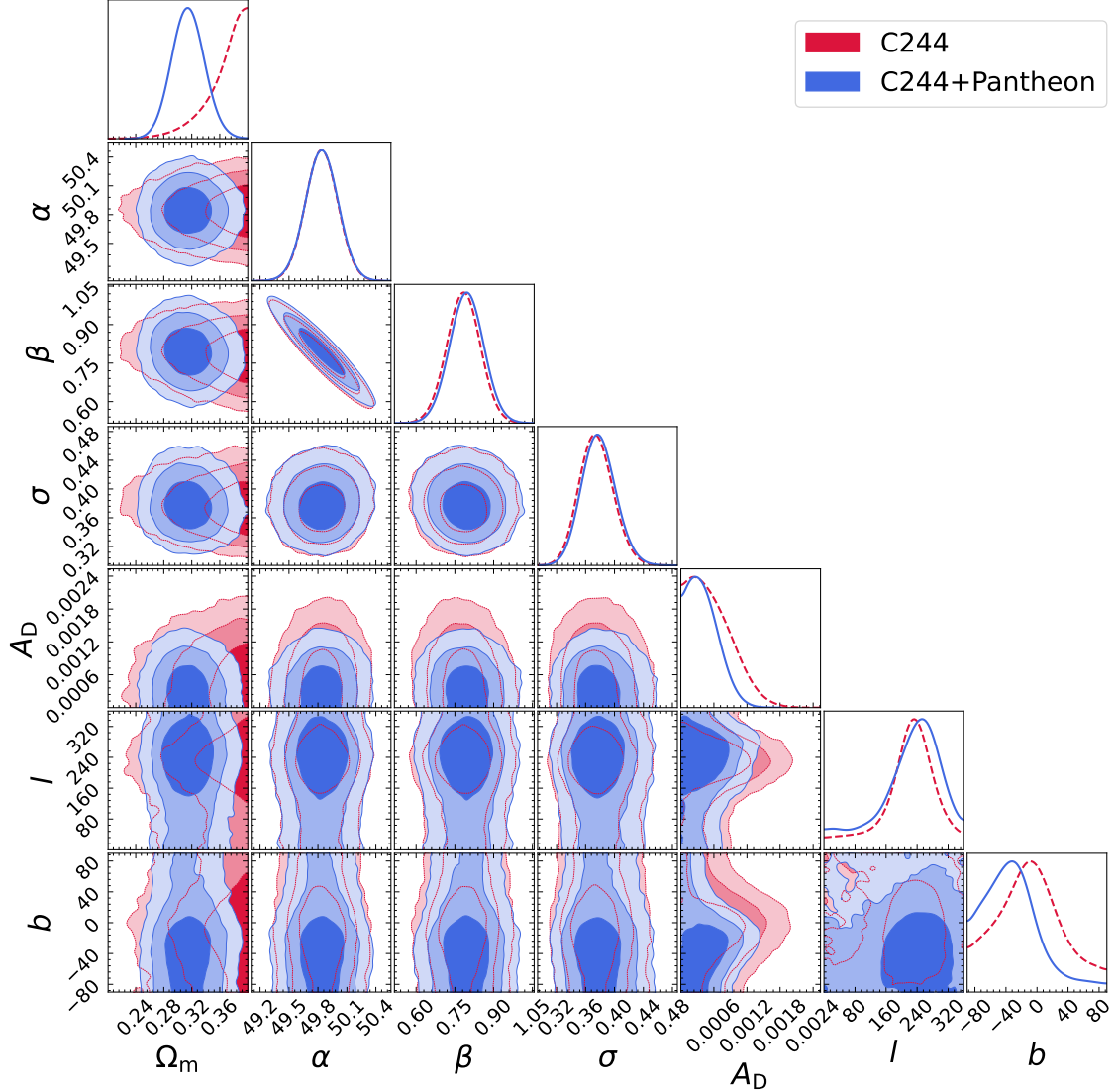


**Fig. 4:** Marginalized posterior distributions of parameters in the dipole-modulated  $\Lambda$ CDM model. The red and blue curves represent the results derived from the C244 and C244+Pantheon samples, respectively.

the “up” and “down” hemispheres are  $\Omega_{m,u} = 0.346 \pm 0.023$  and  $\Omega_{m,d} = 0.266 \pm 0.026$ , respectively.

Table 2 summarizes the results obtained from the joint datasets (C244+Pantheon and A118+Pantheon) and the individual Pantheon sample. The two joint datasets produce highly consistent values for  $AL_{\max}$ . When the Pantheon sample is combined with the two GRB samples,

respectively, the values of  $AL_{\max}$  decrease significantly. Nevertheless, all values of  $AL_{\max}$  are consistent within the  $1\sigma$  uncertainty.

In Figure 8, we plot the preferred direction corresponding to  $AL_{\max}$  along with its  $1\sigma$  uncertainty region. The preferred direction derived from the A118+Pantheon sample is consistent with that from the Pantheon sample within  $1\sigma$  uncertainty. Clearly, the preferred direction from the C244+Pantheon sample does not exhibit such consistency, deviating beyond the  $1\sigma$  uncertainty. As

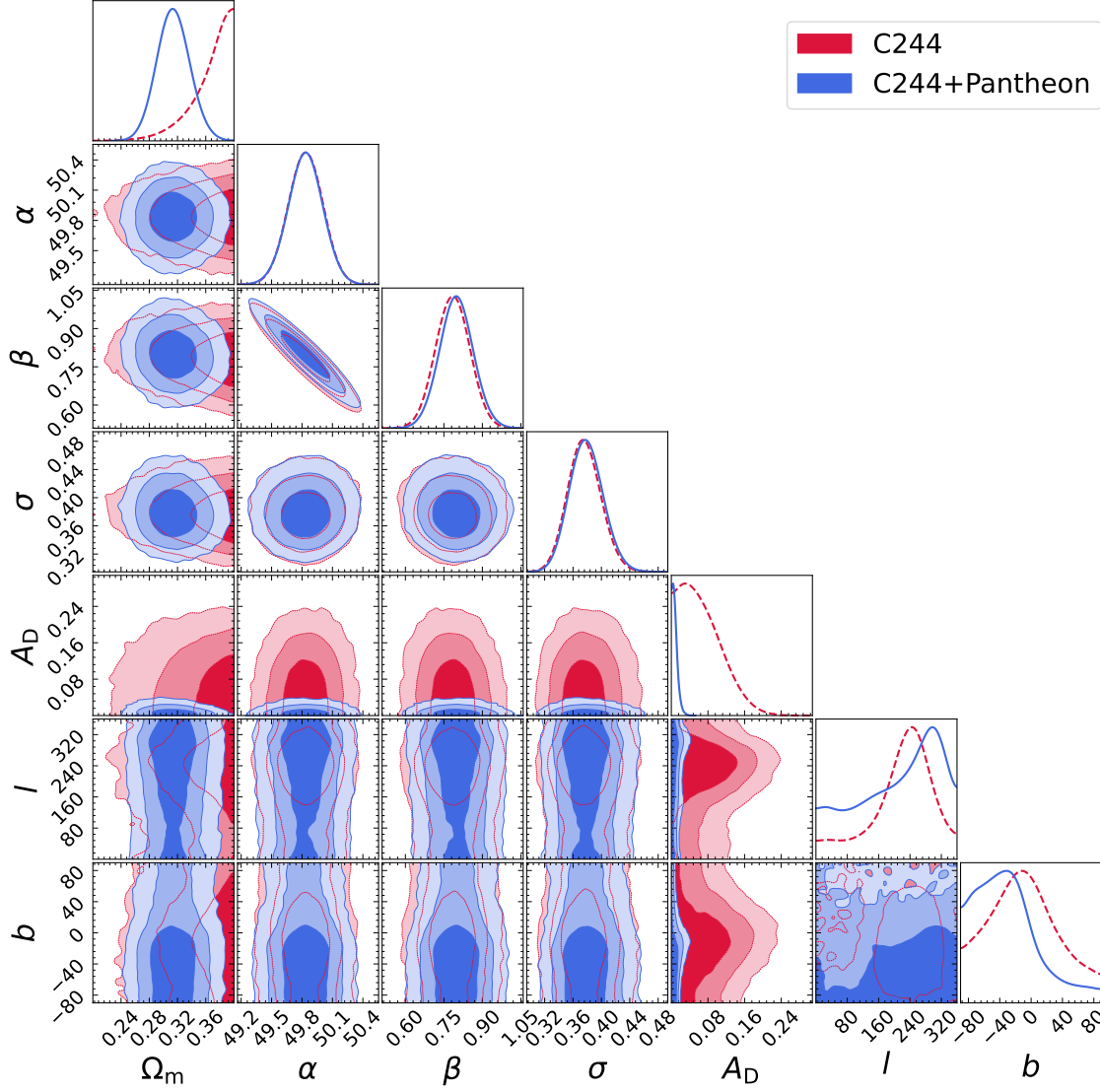
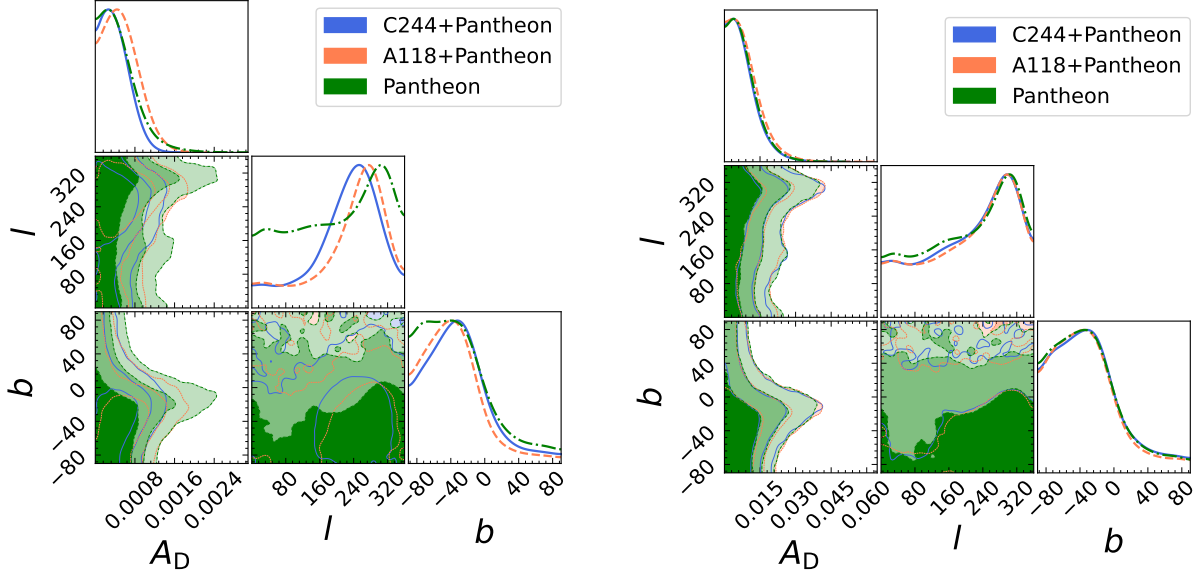


**Fig. 5:** Marginalized posterior distributions of parameters in the Finslerian cosmological model. The red and blue curves represent the results derived from the C244 and C244+Pantheon samples, respectively.

**Table 2:** Results of the HC method obtained from the joint datasets (C244+Pantheon and A118+Pantheon) and the individual Pantheon sample.

Sample	$\Omega_{m,u}$	$\Omega_{m,d}$	$AL_{\max}$	$l[^\circ]$	$b[^\circ]$
C244+Pantheon	$0.346 \pm 0.023$	$0.266 \pm 0.026$	$0.264 \pm 0.057$	$66.45^{+31.29}_{-51.68}$	$-9.59^{+53.00}_{-17.69}$
A118+Pantheon	$0.344 \pm 0.023$	$0.266 \pm 0.028$	$0.257 \pm 0.060$	$82.97^{+52.73}_{-61.88}$	$-15.09^{+60.09}_{-13.54}$
Pantheon	$0.313 \pm 0.023$	$0.217 \pm 0.029$	$0.361 \pm 0.070$	$123.05^{+11.25}_{-4.22}$	$4.78^{+1.80}_{-8.36}$



(a) Anisotropic signals in the dipole-modulated  $\Lambda$ CDM model.

(b) Anisotropic signals in the Finslerian cosmological model.

**Fig. 6:** Marginalized posterior distributions for the parameters of anisotropic signals. Panel (a) shows the results in the dipole-modulated  $\Lambda$ CDM model, and panel (b) shows the results in the Finslerian cosmological model. The blue and green lines denote the results obtained from the C244+Pantheon and Pantheon samples, respectively. The orange lines denote the results obtained from the A118+Pantheon sample, which are taken from our previous work [71].

the number of GRBs increases from 118 to 244, the preferred direction changes significantly.

## 4 Conclusion

We employed the sample of 244 GRBs with the Combo correlation to test the cosmic anisotropy in both the dipole-modulated  $\Lambda$ CDM model and the Finslerian cosmological model. The anisotropic signal in the C244 sample is negligible. By combining the C244 sample with the Pantheon sample, we obtained joint cosmological constraints.

For the DF method, we found that combining the C244 sample with the Pantheon sample in the dipole-modulated  $\Lambda$ CDM model reduces the uncertainty in longitude  $l$  by approximately 40%. Furthermore, the incorporation of the C244 sample leads to the  $54.09^\circ$  shift in the best-fitting longitude  $l$ . Compared with the A118+Pantheon sample, the shift in longitude  $l$  increases by an additional  $21.35^\circ$  as the number of GRBs increases from 118 to 244. In the Finslerian cosmological

model, the dipole directions determined from the C244+Pantheon, A118+Pantheon, and Pantheon samples are highly consistent with each other.

In the HC method, for the C244+Pantheon sample, we found  $AL_{\max} = 0.264 \pm 0.057$  and the corresponding direction is  $(l, b) = (66.45^{+31.29^\circ}_{-51.68^\circ}, -9.59^{+53.00^\circ}_{-17.69^\circ})$ . Compared to the Pantheon-only result, the value of  $AL_{\max}$  decreases significantly. Nevertheless, these two values of  $AL_{\max}$  remain consistent within  $1\sigma$  uncertainty. However, we found that the preferred direction derived from the C244+Pantheon sample deviates from the Pantheon-only result by more than  $1\sigma$ . In contrast, the preferred direction from the A118+Pantheon sample is consistent with the Pantheon-only result within  $1\sigma$  uncertainty. These results confirm that the preferred direction changes significantly as the number of GRBs increases from 118 to 244.

Our results show that GRBs can suppress the fake anisotropic signals induced by inhomogeneous spatial distributions. Therefore, we believe that

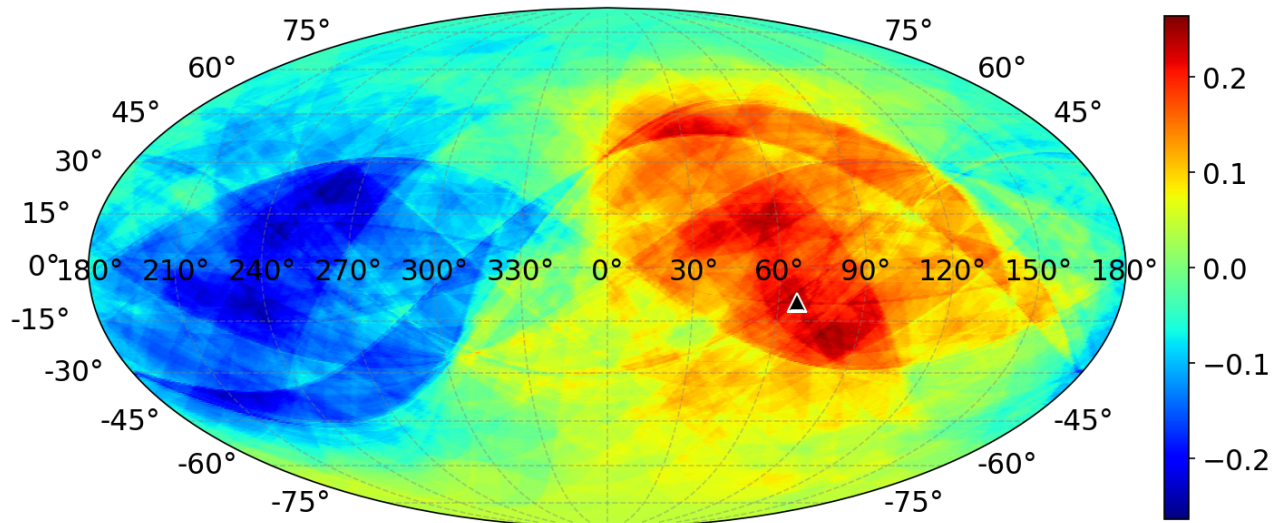


**Fig. 7:** Pseudo-color map of the AL from the C244+Pantheon sample in Galactic coordinates. The triangle marks the position of  $AL_{\max}$ .

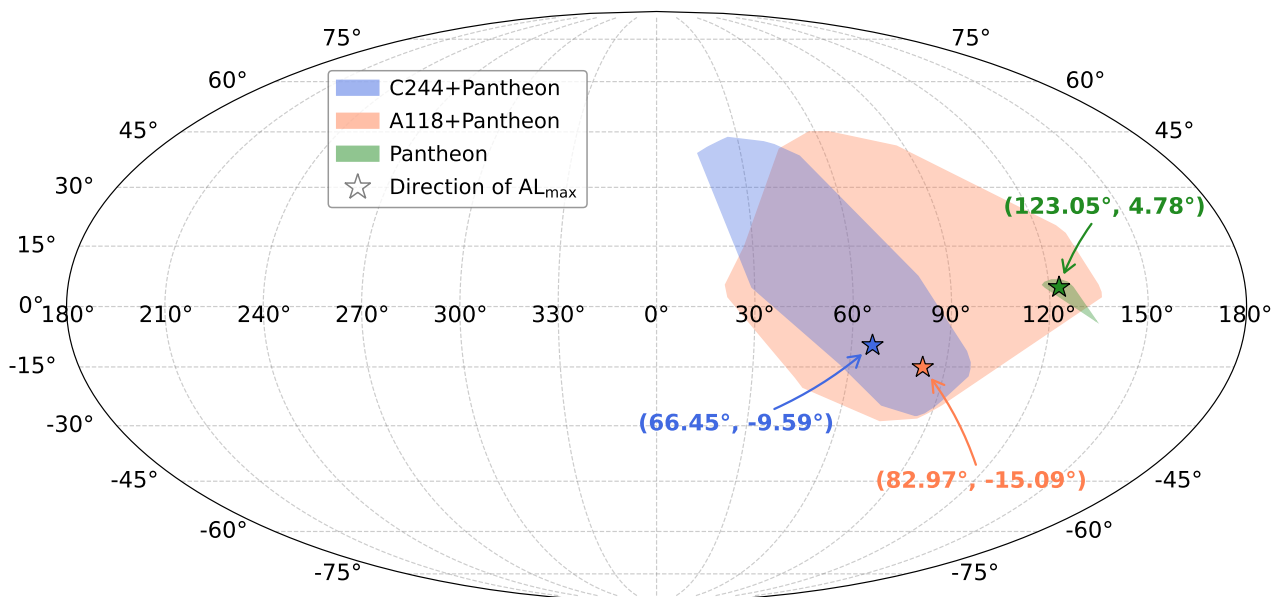


**Fig. 8:** Preferred direction corresponding to  $AL_{\max}$  along with its  $1\sigma$  uncertainty region. The blue, orange, and green shaded areas indicate the results from the C244+Pantheon, A118+Pantheon, and Pantheon samples, respectively. The star markers represent the preferred directions corresponding to  $AL_{\max}$  for each sample.

GRBs have the potential to provide a reliable probe of cosmic anisotropy. Currently, GRBs still face several limitations as cosmological probes, such as limited sample sizes and a shortage of low-redshift sources. Space missions such as the currently successfully operating SVOM [91], along with proposed future missions like THESEUS [92], are expected to provide much larger and more precise GRB samples. These advanced observations will significantly improve the statistical precision of GRB-based cosmological constraints.

**Acknowledgements.** J.-Q.X. is supported by the National Natural Science Foundation of China, under grant Nos. 12473004 and 12021003, the National Key R&D Program of China, No. 2020YFC2201603.

## References

- [1] G. Hinshaw, et al., Nine-Year Wilkinson Microwave Anisotropy Probe (WMAP) Observations: Cosmological Parameter Results. *Astrophys. J. Suppl.* **208**, 19 (2013). <https://doi.org/10.1088/0067-0049/208/2/19>. arXiv:1212.5226 [astro-ph.CO]
- [2] N. Aghanim, et al., Planck 2018 results. VI. Cosmological parameters. *Astron. Astrophys.* **641**, A6 (2020). <https://doi.org/10.1051/0004-6361/201833910>. [Erratum: *Astron. Astrophys.* 652, C4 (2021)]. arXiv:1807.06209 [astro-ph.CO]
- [3] Y. Akrami, et al., Planck 2018 results. VII. Isotropy and Statistics of the CMB. *Astron. Astrophys.* **641**, A7 (2020). <https://doi.org/10.1051/0004-6361/201935201>. arXiv:1906.02552 [astro-ph.CO]
- [4] J. Kim, P. Naselsky, Anomalous parity asymmetry of the Wilkinson Microwave Anisotropy Probe power spectrum data at low multipoles. *Astrophys. J. Lett.* **714**, L265–L267 (2010). <https://doi.org/10.1088/2041-8205/714/2/L265>. arXiv:1001.4613 [astro-ph.CO]
- [5] A. Gruppuso, F. Finelli, P. Natoli, F. Paci, P. Cabella, A. De Rosa, N. Mandolesi, New constraints on Parity Symmetry from a re-analysis of the WMAP-7 low resolution power spectra. *Mon. Not. Roy. Astron. Soc.* **411**, 1445–1452 (2011). <https://doi.org/10.1111/j.1365-2966.2010.17773.x>. arXiv:1006.1979 [astro-ph.CO]
- [6] W. Zhao, Directional dependence of CMB parity asymmetry. *Phys. Rev. D* **89**(2), 023010 (2014). <https://doi.org/10.1103/PhysRevD.89.023010>. arXiv:1306.0955 [astro-ph.CO]
- [7] D. Hutsemekers, R. Cabanac, H. Lamy, D. Sluse, Mapping extreme-scale alignments of quasar polarization vectors. *Astron. Astrophys.* **441**, 915–930 (2005). <https://doi.org/10.1051/0004-6361:20053337>. arXiv:astro-ph/0507274
- [8] V. Pelgrims, D. Hutsemekers, Evidence for the alignment of quasar radio polarizations with large quasar group axes. *Astron. Astrophys.* **590**, A53 (2016). <https://doi.org/10.1051/0004-6361/201526979>. arXiv:1604.03937 [astro-ph.GA]
- [9] R. Amanullah, et al., Spectra and Light Curves of Six Type Ia Supernovae at  $0.511 < z < 1.12$  and the Union2 Compilation. *Astrophys. J.* **716**, 712–738 (2010). <https://doi.org/10.1088/0004-637X/716/1/712>. arXiv:1004.1711 [astro-ph.CO]
- [10] N. Suzuki, et al., The Hubble Space Telescope Cluster Supernova Survey: V. Improving the Dark Energy Constraints Above  $z > 1$  and Building an Early-Type-Hosted Supernova Sample. *Astrophys. J.* **746**, 85 (2012). <https://doi.org/10.1088/0004-637X/746/1/85>. arXiv:1105.3470 [astro-ph.CO]
- [11] M. Betoule, et al., Improved cosmological constraints from a joint analysis of the SDSS-II and SNLS supernova samples. *Astron. Astrophys.* **568**, A22 (2014). <https://doi.org/10.1051/0004-6361/201423413>. arXiv:1401.4064 [astro-ph.CO]
- [12] D.M. Scolnic, et al., The Complete Light-curve Sample of Spectroscopically Confirmed SNe Ia from Pan-STARRS1 and Cosmological Constraints from the Combined Pantheon Sample. *Astrophys. J.* **859**(2), 101

- (2018). <https://doi.org/10.3847/1538-4357/aab9bb>. arXiv:1710.00845 [astro-ph.CO]
- [13] D. Scolnic, et al., The Pantheon+ Analysis: The Full Data Set and Light-curve Release. *Astrophys. J.* **938**(2), 113 (2022). <https://doi.org/10.3847/1538-4357/ac8b7a>. arXiv:2112.03863 [astro-ph.CO]
- [14] A. Mariano, L. Perivolaropoulos, Is there correlation between Fine Structure and Dark Energy Cosmic Dipoles? *Phys. Rev. D* **86**, 083517 (2012). <https://doi.org/10.1103/PhysRevD.86.083517>. arXiv:1206.4055 [astro-ph.CO]
- [15] W. Zhao, P.X. Wu, Y. Zhang, Anisotropy of Cosmic Acceleration. *Int. J. Mod. Phys. D* **22**, 1350060 (2013). <https://doi.org/10.1142/S0218271813500600>. arXiv:1305.2701 [astro-ph.CO]
- [16] X. Yang, F.Y. Wang, Z. Chu, Searching for a preferred direction with Union2.1 data. *Mon. Not. Roy. Astron. Soc.* **437**(2), 1840–1846 (2014). <https://doi.org/10.1093/mnras/stt2015>. arXiv:1310.5211 [astro-ph.CO]
- [17] X. Li, H.N. Lin, S. Wang, Z. Chang, A unified description for dipoles of the fine-structure constant and SnIa Hubble diagram in Finslerian universe. *Eur. Phys. J. C* **75**(5), 181 (2015). <https://doi.org/10.1140/epjc/s10052-015-3380-2>. arXiv:1501.06738 [gr-qc]
- [18] H.N. Lin, X. Li, Z. Chang, The significance of anisotropic signals hiding in the type Ia supernovae. *Mon. Not. Roy. Astron. Soc.* **460**(1), 617–626 (2016). <https://doi.org/10.1093/mnras/stw995>. arXiv:1604.07505 [astro-ph.CO]
- [19] Z.Q. Sun, F.Y. Wang, Probing the isotropy of cosmic acceleration using different supernova samples. *Eur. Phys. J. C* **79**(9), 783 (2019). <https://doi.org/10.1140/epjc/s10052-019-7293-3>. arXiv:1804.05191 [astro-ph.CO]
- [20] H.N. Lin, S. Wang, Z. Chang, X. Li, Testing the isotropy of the Universe by using the JLA compilation of type-Ia supernovae. *Mon. Not. Roy. Astron. Soc.* **456**(2), 1881–1885 (2016). <https://doi.org/10.1093/mnras/stv2804>. arXiv:1504.03428 [astro-ph.CO]
- [21] Y.Y. Wang, F.Y. Wang, Testing the isotropy of the Universe with type Ia supernovae in a model-independent way. *Mon. Not. Roy. Astron. Soc.* **474**(3), 3516–3522 (2018). <https://doi.org/10.1093/mnras/stx2982>. arXiv:1711.05974 [astro-ph.CO]
- [22] Z. Chang, H.N. Lin, Y. Sang, S. Wang, A tomographic test of cosmological principle using the JLA compilation of type Ia supernovae. *Mon. Not. Roy. Astron. Soc.* **478**(3), 3633–3639 (2018). <https://doi.org/10.1093/mnras/sty1120>. arXiv:1711.11321 [astro-ph.CO]
- [23] Z.Q. Sun, F.Y. Wang, Testing the anisotropy of cosmic acceleration from Pantheon supernovae sample. *Mon. Not. Roy. Astron. Soc.* **478**(4), 5153–5158 (2018). <https://doi.org/10.1093/mnras/sty1391>. arXiv:1805.09195 [astro-ph.CO]
- [24] H.K. Deng, H. Wei, Null signal for the cosmic anisotropy in the Pantheon supernovae data. *Eur. Phys. J. C* **78**(9), 755 (2018). <https://doi.org/10.1140/epjc/s10052-018-6159-4>. arXiv:1806.02773 [astro-ph.CO]
- [25] D. Zhao, Y. Zhou, Z. Chang, Anisotropy of the Universe via the Pantheon supernovae sample revisited. *Mon. Not. Roy. Astron. Soc.* **486**(4), 5679–5689 (2019). <https://doi.org/10.1093/mnras/stz1259>. arXiv:1903.12401 [astro-ph.CO]
- [26] Z. Chang, D. Zhao, Y. Zhou, Constraining the anisotropy of the Universe with the Pantheon supernovae sample. *Chin. Phys. C* **43**(12), 125102 (2019). <https://doi.org/10.1088/1674-1137/43/12/125102>. arXiv:1910.06883 [astro-ph.CO]
- [27] L. Tang, H.N. Lin, L. Liu, X. Li, Consistency of Pantheon+ supernovae with a large-scale isotropic universe\*. *Chin. Phys. C* **47**(12), 125101 (2023). <https://doi.org/10.1088/1674-1137/acfaf0>. arXiv:2309.11320

- [astro-ph.CO]
- [28] F. Sorrenti, R. Durrer, M. Kunz, The dipole of the Pantheon+SH0ES data. *JCAP* **11**, 054 (2023). <https://doi.org/10.1088/1475-7516/2023/11/054>. [arXiv:2212.10328](https://arxiv.org/abs/2212.10328) [astro-ph.CO]
- [29] J.A. Cowell, S. Dhawan, H.J. Macpherson, Potential signature of a quadrupolar hubble expansion in Pantheon+supernovae. *Mon. Not. Roy. Astron. Soc.* **526**(1), 1482–1494 (2023). <https://doi.org/10.1093/mnras/stad2788>. [arXiv:2212.13569](https://arxiv.org/abs/2212.13569) [astro-ph.CO]
- [30] F. Sorrenti, R. Durrer, M. Kunz, A local infall from a cosmographic analysis of Pantheon+. *JCAP* **12**, 003 (2024). <https://doi.org/10.1088/1475-7516/2024/12/003>. [arXiv:2407.07002](https://arxiv.org/abs/2407.07002) [astro-ph.CO]
- [31] A. Sah, M. Rameez, S. Sarkar, C.G. Tsagas, Anisotropy in Pantheon+ supernovae. *Eur. Phys. J. C* **85**(5), 596 (2025). <https://doi.org/10.1140/epjc/s10052-025-14222-w>. [arXiv:2411.10838](https://arxiv.org/abs/2411.10838) [astro-ph.CO]
- [32] J.P. Hu, Y.Y. Wang, J. Hu, F.Y. Wang, Testing the cosmological principle with the Pantheon+ sample and the region-fitting method. *Astron. Astrophys.* **681**, A88 (2024). <https://doi.org/10.1051/0004-6361/202347121>. [arXiv:2310.11727](https://arxiv.org/abs/2310.11727) [astro-ph.CO]
- [33] J. Hu, J. Hu, X. Jia, B. Gao, F. Wang, Testing cosmic anisotropy with Padé approximations and the latest Pantheon+ sample. *Astron. Astrophys.* **689**, A215 (2024). <https://doi.org/10.1051/0004-6361/202450342>. [arXiv:2406.14827](https://arxiv.org/abs/2406.14827) [astro-ph.CO]
- [34] L. Perivolaropoulos, Isotropy properties of the absolute luminosity magnitudes of SnIa in the Pantheon+ and SH0ES samples. *Phys. Rev. D* **108**(6), 063509 (2023). <https://doi.org/10.1103/PhysRevD.108.063509>. [arXiv:2305.12819](https://arxiv.org/abs/2305.12819) [astro-ph.CO]
- [35] C.A.P. Bengaly, J.S. Alcaniz, C. Pigozzo, Testing the isotropy of cosmic acceleration with the Pantheon+ and SH0ES datasets: A cosmographic analysis. *Phys. Rev. D* **109**(12), 123533 (2024). <https://doi.org/10.1103/PhysRevD.109.123533>. [arXiv:2402.17741](https://arxiv.org/abs/2402.17741) [astro-ph.CO]
- [36] A.J. Zhou, S. Dodelson, D. Scolnic, Isotropy of Hubble Expansion in the Early and Late Universe. *Phys. Rev. Lett.* **135**(26), 261002 (2025). <https://doi.org/10.1103/w99g-lgmn>. [arXiv:2506.14878](https://arxiv.org/abs/2506.14878) [astro-ph.CO]
- [37] P. Boubel, M. Colless, K. Said, L. Staveley-Smith, Testing anisotropic Hubble expansion. *JCAP* **03**, 066 (2025). <https://doi.org/10.1088/1475-7516/2025/03/066>. [arXiv:2412.14607](https://arxiv.org/abs/2412.14607) [astro-ph.CO]
- [38] R. Stiskalek, H. Desmond, G. Lavaux, No evidence for local H0 anisotropy from Tully–Fisher or supernova distances. *Mon. Not. Roy. Astron. Soc.* **546**(2), staf2048 (2026). <https://doi.org/10.1093/mnras/staf2048>. [arXiv:2509.14997](https://arxiv.org/abs/2509.14997) [astro-ph.CO]
- [39] K. Migkas, T.H. Reiprich, Anisotropy of the galaxy cluster X-ray luminosity–temperature relation. *Astron. Astrophys.* **611**, A50 (2018). <https://doi.org/10.1051/0004-6361/201731222>. [arXiv:1711.02539](https://arxiv.org/abs/1711.02539) [astro-ph.CO]
- [40] K. Migkas, G. Schellenberger, T.H. Reiprich, F. Pacaud, M.E. Ramos-Ceja, L. Lovisari, Probing cosmic isotropy with a new X-ray galaxy cluster sample through the  $L_X - T$  scaling relation. *Astron. Astrophys.* **636**, A15 (2020). <https://doi.org/10.1051/0004-6361/201936602>. [arXiv:2004.03305](https://arxiv.org/abs/2004.03305) [astro-ph.CO]
- [41] K. Migkas, F. Pacaud, G. Schellenberger, J. Erler, N.T. Nguyen-Dang, T.H. Reiprich, M.E. Ramos-Ceja, L. Lovisari, Cosmological implications of the anisotropy of ten galaxy cluster scaling relations. *Astron. Astrophys.* **649**, A151 (2021). <https://doi.org/10.1051/0004-6361/202140296>. [arXiv:2103.13904](https://arxiv.org/abs/2103.13904) [astro-ph.CO]
- [42] P.K. Aluri, et al., Is the observable Universe consistent with the cosmological principle? *Class. Quant. Grav.* **40**(9), 094001 (2023). <https://doi.org/10.1088/1361-6382/acbefc>. [arXiv:2207.05765](https://arxiv.org/abs/2207.05765) [astro-ph.CO]

- [43] A. Pandya, K. Migkas, T.H. Reiprich, A. Stanford, F. Pacaud, G. Schellenberger, L. Lovisari, M.E. Ramos-Ceja, N.T. Nguyen-Dang, S. Park, Examining the local Universe isotropy with galaxy cluster velocity dispersion scaling relations. *Astron. Astrophys.* **691**, A355 (2024). <https://doi.org/10.1051/0004-6361/202451755>. [arXiv:2408.00726](https://arxiv.org/abs/2408.00726) [astro-ph.CO]
- [44] R.G. Cai, T.B. Liu, S.J. Wang, W.T. Xu, Probing cosmic anisotropy with GW/FRB as upgraded standard sirens. *JCAP* **09**, 016 (2019). <https://doi.org/10.1088/1475-7516/2019/09/016>. [arXiv:1905.01803](https://arxiv.org/abs/1905.01803) [astro-ph.CO]
- [45] B. Cousins, A. Dhani, B.S. Sathyaprakash, N. Yunes, Finding cosmic anisotropy with networks of next-generation gravitational-wave detectors. *Phys. Rev. D* **111**(10), 103530 (2025). <https://doi.org/10.1103/PhysRevD.111.103530>. [arXiv:2406.15550](https://arxiv.org/abs/2406.15550) [gr-qc]
- [46] A. Chen, Measuring the cosmic dipole with golden dark sirens in the era of next-generation ground-based gravitational wave detectors. *JCAP* **07**, 076 (2025). <https://doi.org/10.1088/1475-7516/2025/07/076>. [arXiv:2505.12678](https://arxiv.org/abs/2505.12678) [gr-qc]
- [47] X. Wang, Z. Huang, Testing the cosmological principle on gigaparsec scales. *JCAP* **02**, 031 (2026). <https://doi.org/10.1088/1475-7516/2026/02/031>. [arXiv:2505.19055](https://arxiv.org/abs/2505.19055) [astro-ph.CO]
- [48] D.C. Qiang, H.K. Deng, H. Wei, Cosmic Anisotropy and Fast Radio Bursts. *Class. Quant. Grav.* **37**(18), 185022 (2020). <https://doi.org/10.1088/1361-6382/ab7f8e>. [arXiv:1902.03580](https://arxiv.org/abs/1902.03580) [astro-ph.CO]
- [49] H.N. Lin, Y. Sang, Probing the anisotropic distribution of baryon matter in the Universe using fast radio bursts \*. *Chin. Phys. C* **45**(12), 125101 (2021). <https://doi.org/10.1088/1674-1137/ac2660>. [arXiv:2111.12934](https://arxiv.org/abs/2111.12934) [astro-ph.CO]
- [50] N.J. Secrest, S. von Hausegger, M. Rameez, R. Mohayaee, S. Sarkar, J. Colin, A Test of the Cosmological Principle with Quasars. *Astrophys. J. Lett.* **908**(2), L51 (2021). <https://doi.org/10.3847/2041-8213/abdd40>. [arXiv:2009.14826](https://arxiv.org/abs/2009.14826) [astro-ph.CO]
- [51] N.J. Secrest, S. von Hausegger, M. Rameez, R. Mohayaee, S. Sarkar, A Challenge to the Standard Cosmological Model. *Astrophys. J. Lett.* **937**(2), L31 (2022). <https://doi.org/10.3847/2041-8213/ac88c0>. [arXiv:2206.05624](https://arxiv.org/abs/2206.05624) [astro-ph.CO]
- [52] L. Dam, G.F. Lewis, B.J. Brewer, Testing the cosmological principle with CatWISE quasars: a bayesian analysis of the number-count dipole. *Mon. Not. Roy. Astron. Soc.* **525**(1), 231–245 (2023). <https://doi.org/10.1093/mnras/stad2322>. [arXiv:2212.07733](https://arxiv.org/abs/2212.07733) [astro-ph.CO]
- [53] C. Guandalin, J. Piat, C. Clarkson, R. Maartens, Theoretical Systematics in Testing the Cosmological Principle with the Kinematic Quasar Dipole. *Astrophys. J.* **953**(2), 144 (2023). <https://doi.org/10.3847/1538-4357/acdf46>. [arXiv:2212.04925](https://arxiv.org/abs/2212.04925) [astro-ph.CO]
- [54] A.K. Singal, Discordance of dipole asymmetries seen in recent large radio surveys with the cosmological principle. *Mon. Not. Roy. Astron. Soc.* **524**(3), 3636–3646 (2023). <https://doi.org/10.1093/mnras/stad2161>. [arXiv:2303.05141](https://arxiv.org/abs/2303.05141) [astro-ph.CO]
- [55] J.D. Wagnveld, H.R. Klöckner, D.J. Schwarz, The cosmic radio dipole: Bayesian estimators on new and old radio surveys. *Astron. Astrophys.* **675**, A72 (2023). <https://doi.org/10.1051/0004-6361/202346210>. [arXiv:2305.15335](https://arxiv.org/abs/2305.15335) [astro-ph.CO]
- [56] Y.T. Cheng, T.C. Chang, A. Lidz, Is the Radio Source Dipole from NVSS Consistent with the Cosmic Microwave Background and  $\Lambda$ CDM? *Astrophys. J.* **965**(1), 32 (2024). <https://doi.org/10.3847/1538-4357/ad28bf>. [arXiv:2309.02490](https://arxiv.org/abs/2309.02490) [astro-ph.CO]

- [57] M. Panwar, P. Jain, Probing the cosmological principle using the slope of  $\log N$ - $\log S$  relationship for quasars. *JCAP* **06**, 019 (2024). <https://doi.org/10.1088/1475-7516/2024/06/019>. [arXiv:2312.07596](https://arxiv.org/abs/2312.07596) [astro-ph.CO]
- [58] A.K. Singal, Resolution of the incongruency of dipole asymmetries within various large radio surveys – implications for the Cosmological Principle. *Mon. Not. Roy. Astron. Soc.* **528**(4), 5679–5691 (2024). <https://doi.org/10.1093/mnras/stae414>. [arXiv:2312.12785](https://arxiv.org/abs/2312.12785) [astro-ph.CO]
- [59] P. da Silveira Ferreira, V. Marra, Tomographic redshift dipole: testing the cosmological principle. *JCAP* **09**, 077 (2024). <https://doi.org/10.1088/1475-7516/2024/09/077>. [arXiv:2403.14580](https://arxiv.org/abs/2403.14580) [astro-ph.CO]
- [60] A.K. Singal, Cosmic dipoles of active galactic nuclei at optical and radio wavelengths display much larger amplitudes than the cosmic microwave background dipole. *Mon. Not. Roy. Astron. Soc.* **532**(1), L1–L6 (2024). <https://doi.org/10.1093/mnras/slae039>. [arXiv:2403.16581](https://arxiv.org/abs/2403.16581) [astro-ph.CO]
- [61] A. Abghari, E.F. Bunn, L.T. Hergt, B. Li, D. Scott, R.M. Sullivan, D. Wei, Reassessment of the dipole in the distribution of quasars on the sky. *JCAP* **11**, 067 (2024). <https://doi.org/10.1088/1475-7516/2024/11/067>. [arXiv:2405.09762](https://arxiv.org/abs/2405.09762) [astro-ph.CO]
- [62] P. Tiwari, D.J. Schwarz, G.B. Zhao, R. Durrer, M. Kunz, H. Padmanabhan, An Independent Measure of the Kinematic Dipole from SDSS. *Astrophys. J.* **975**(2), 279 (2024). <https://doi.org/10.3847/1538-4357/ad815b>. [arXiv:2409.09946](https://arxiv.org/abs/2409.09946) [astro-ph.CO]
- [63] J.D. Wagenfeld, S. von Hausegger, H.R. Klöckner, D.J. Schwarz, The kinematic contribution to the cosmic number count dipole. *Astron. Astrophys.* **697**, A112 (2025). <https://doi.org/10.1051/0004-6361/202453397>. [arXiv:2503.02470](https://arxiv.org/abs/2503.02470) [astro-ph.CO]
- [64] J.P. Hu, Y.Y. Wang, F.Y. Wang, Testing cosmic anisotropy with Pantheon sample and quasars at high redshifts. *Astron. Astrophys.* **643**, A93 (2020). <https://doi.org/10.1051/0004-6361/202038541>. [arXiv:2008.12439](https://arxiv.org/abs/2008.12439) [astro-ph.CO]
- [65] D. Zhao, J.Q. Xia, Constraining the anisotropy of the Universe with the X-ray and UV fluxes of quasars. *Eur. Phys. J. C* **81**(8), 694 (2021). <https://doi.org/10.1140/epjc/s10052-021-09491-0>. [arXiv:2105.03965](https://arxiv.org/abs/2105.03965) [astro-ph.CO]
- [66] D. Zhao, J.Q. Xia, A tomographic test of cosmic anisotropy with the recently-released quasar sample. *Eur. Phys. J. C* **81**(10), 948 (2021). <https://doi.org/10.1140/epjc/s10052-021-09701-9>
- [67] M.H. Li, H.N. Lin, Testing the homogeneity of the Universe using gamma-ray bursts. *Astron. Astrophys.* **582**, A111 (2015). <https://doi.org/10.1051/0004-6361/201525736>. [arXiv:1509.03027](https://arxiv.org/abs/1509.03027) [astro-ph.CO]
- [68] Z. Chang, X. Li, H.N. Lin, S. Wang, Constraining the Anisotropy of the Universe from Supernovae and Gamma-ray Bursts. *Mod. Phys. Lett. A* **29**(15), 1450067 (2014). <https://doi.org/10.1142/S0217732314500679>. [arXiv:1405.3074](https://arxiv.org/abs/1405.3074) [astro-ph.CO]
- [69] J.S. Wang, F.Y. Wang, Probing the anisotropic expansion from supernovae and GRBs in a model-independent way. *Mon. Not. Roy. Astron. Soc.* **443**(2), 1680–1687 (2014). <https://doi.org/10.1093/mnras/stu1279>. [arXiv:1406.6448](https://arxiv.org/abs/1406.6448) [astro-ph.CO]
- [70] O. Luongo, M. Muccino, E.Ó. Colgáin, M.M. Sheikh-Jabbari, L. Yin, Larger  $H_0$  values in the CMB dipole direction. *Phys. Rev. D* **105**(10), 103510 (2022). <https://doi.org/10.1103/PhysRevD.105.103510>. [arXiv:2108.13228](https://arxiv.org/abs/2108.13228) [astro-ph.CO]
- [71] D. Zhao, J.Q. Xia, Testing cosmic anisotropy with the  $E_p$ – $E_{iso}$  (‘Amati’) correlation of GRBs. *Mon. Not. Roy. Astron. Soc.* **511**(4), 5661–5671 (2022). <https://doi.org/10.1093>

- [72] O. Luongo, M. Muccino, F. Sorrenti, Exploring the cosmic microwave background dipole direction using gamma-ray bursts. *Astron. Astrophys.* **703**, A115 (2025). <https://doi.org/10.1051/0004-6361/202556806>. [arXiv:2508.04304](https://arxiv.org/abs/2508.04304) [astro-ph.CO]
- [73] J. Santiago, K. Asvesta, M.G. Dainotti, P. Chen, Measuring cosmic dipole with the GRB luminosity-time relation. *JHEAp* **51**, 100554 (2026). <https://doi.org/10.1016/j.jheap.2026.100554>. [arXiv:2510.20705](https://arxiv.org/abs/2510.20705) [astro-ph.CO]
- [74] G. Risaliti, E. Lusso, A Hubble Diagram for Quasars. *Astrophys. J.* **815**, 33 (2015). <https://doi.org/10.1088/0004-637X/815/1/33>. [arXiv:1505.07118](https://arxiv.org/abs/1505.07118) [astro-ph.CO]
- [75] G. Risaliti, E. Lusso, Cosmological constraints from the Hubble diagram of quasars at high redshifts. *Nature Astron.* **3**(3), 272–277 (2019). <https://doi.org/10.1038/s41550-018-0657-z>. [arXiv:1811.02590](https://arxiv.org/abs/1811.02590) [astro-ph.CO]
- [76] E. Lusso, et al., Quasars as standard candles III. Validation of a new sample for cosmological studies. *Astron. Astrophys.* **642**, A150 (2020). <https://doi.org/10.1051/0004-6361/202038899>. [arXiv:2008.08586](https://arxiv.org/abs/2008.08586) [astro-ph.GA]
- [77] A. Cucchiara, et al., A Photometric Redshift of  $z \sim 9.4$  for GRB 090429B. *Astrophys. J.* **736**, 7 (2011). <https://doi.org/10.1088/0004-637X/736/1/7>. [arXiv:1105.4915](https://arxiv.org/abs/1105.4915) [astro-ph.CO]
- [78] P. D’Avanzo, et al., A complete sample of bright Swift Gamma-Ray Bursts: X-ray afterglow luminosity and its correlation with the prompt emission. *Mon. Not. Roy. Astron. Soc.* **425**, 506 (2012). <https://doi.org/10.1111/j.1365-2966.2012.21489.x>. [arXiv:1206.2357](https://arxiv.org/abs/1206.2357) [astro-ph.HE]
- [79] D. Coward, E. Howell, M. Branchesi, G. Strata, D. Guetta, B. Gendre, D. Macpherson, The Swift Gamma-Ray Burst redshift distribution: selection biases and optical brightness evolution at high- $z$ ? *Mon. Not. Roy. Astron. Soc.* **432**, 2141 (2013). <https://doi.org/10.1093/mnras/stt537>. [arXiv:1210.2488](https://arxiv.org/abs/1210.2488) [astro-ph.CO]
- [80] L. Amati, R. D’Agostino, O. Luongo, M. Muccino, M. Tantalò, Addressing the circularity problem in the  $E_p - E_{\text{iso}}$  correlation of gamma-ray bursts. *Mon. Not. Roy. Astron. Soc.* **486**(1), L46–L51 (2019). <https://doi.org/10.1093/mnrasl/slz056>. [arXiv:1811.08934](https://arxiv.org/abs/1811.08934) [astro-ph.HE]
- [81] F.F. Dirirsa, S. Razzaque, F. Piron, M. Arimoto, M. Axelsson, D. Kocevski, F. Longo, M. Ohno, S. Zhu, Spectral analysis of Fermi-LAT gamma-ray bursts with known redshift and their potential use as cosmological standard candles. *Astrophys. J.* **887**, 13 (2019). <https://doi.org/10.3847/1538-4357/ab4e11>. [arXiv:1910.07009](https://arxiv.org/abs/1910.07009) [astro-ph.HE]
- [82] N. Khadka, O. Luongo, M. Muccino, B. Ratra, Do gamma-ray burst measurements provide a useful test of cosmological models? *JCAP* **09**, 042 (2021). <https://doi.org/10.1088/1475-7516/2021/09/042>. [arXiv:2105.12692](https://arxiv.org/abs/2105.12692) [astro-ph.CO]
- [83] M. Muccino, M. Della Valle, L. Izzo, O. Luongo, No evidence for dynamical dark energy from the Combo correlation of GRBs (2026). [arXiv:2604.01980](https://arxiv.org/abs/2604.01980) [astro-ph.CO]
- [84] L. Izzo, M. Muccino, E. Zaninoni, L. Amati, M. Della Valle, New measurements of  $\Omega_m$  from gamma-ray bursts. *Astron. Astrophys.* **582**, A115 (2015). <https://doi.org/10.1051/0004-6361/201526461>. [arXiv:1508.05898](https://arxiv.org/abs/1508.05898) [astro-ph.CO]
- [85] M. Muccino, L. Izzo, O. Luongo, K. Boshkayev, L. Amati, M. Della Valle, G.B. Pisani, E. Zaninoni, Tracing dark energy history with gamma ray bursts. *Astrophys. J.* **908**(2), 181 (2021). <https://doi.org/10.3847/1538-4357/abd254>. [arXiv:2012.03392](https://arxiv.org/abs/2012.03392) [astro-ph.CO]
- [86] G. D’Agostini, Fits, and especially linear fits, with errors on both axes, extra variance of the

data points and other complications (2005).  
[arXiv:physics/0511182](https://arxiv.org/abs/physics/0511182)

- [87] D.J. Schwarz, B. Weinhorst, (An)isotropy of the Hubble diagram: Comparing hemispheres. *Astron. Astrophys.* **474**, 717–729 (2007). <https://doi.org/10.1051/0004-6361:20077998>. [arXiv:0706.0165](https://arxiv.org/abs/astro-ph/0706.0165) [astro-ph]
- [88] D. Foreman-Mackey, D.W. Hogg, D. Lang, J. Goodman, emcee: The MCMC Hammer. *Publ. Astron. Soc. Pac.* **125**, 306–312 (2013). <https://doi.org/10.1086/670067>. [arXiv:1202.3665](https://arxiv.org/abs/1202.3665) [astro-ph.IM]
- [89] K.M. Górski, E. Hivon, A.J. Banday, B.D. Wandelt, F.K. Hansen, M. Reinecke, M. Bartelmann, HEALPix - A Framework for high resolution discretization, and fast analysis of data distributed on the sphere. *Astrophys. J.* **622**, 759–771 (2005). <https://doi.org/10.1086/427976>. [arXiv:astro-ph/0409513](https://arxiv.org/abs/astro-ph/0409513)
- [90] A. Zonca, L. Singer, D. Lenz, M. Reinecke, C. Rosset, E. Hivon, K. Gorski, healpy: equal area pixelization and spherical harmonics transforms for data on the sphere in Python. *J. Open Source Softw.* **4**(35), 1298 (2019). <https://doi.org/10.21105/joss.01298>
- [91] M.G. Bernardini, B. Cordier, J. Wei, The SVOM Mission. *Galaxies* **9**, 113 (2021). <https://doi.org/10.3390/galaxies9040113>. [arXiv:2203.10962](https://arxiv.org/abs/2203.10962) [astro-ph.IM]
- [92] L. Amati, E. Bozzo, D. Götz, P. O’Brien, M. Della Valle, The THESEUS Workshop 2017. *Mem. Soc. Ast. It.* **89**(2), 118–129 (2018). [arXiv:1802.01673](https://arxiv.org/abs/1802.01673) [astro-ph.HE]